

**INDOOR POLLUTANT MIXING TIME IN AN ISOTHERMAL CLOSED
ROOM: AN INVESTIGATION USING CFD**

A.J. Gadgil¹, C. Lobscheid^{1,2} M.O. Abadie^{1,3} and E. U. Finlayson¹

¹Indoor Environment Department, Lawrence Berkeley National Laboratory,
Berkeley, CA 94702, USA

²Current Address: Advent Engineering Services, San Ramon, CA

³Current Address: University of La Rochelle, La Rochelle, France

E-mail of corresponding author: ajgadgil@lbl.gov,

Abstract

We report on computational fluid dynamics (CFD) predictions of mixing time of a pollutant in an unventilated, mechanically-mixed, isothermal room. The study aims to determine: (1) the adequacy of the standard Reynolds Averaged Navier Stokes (RANS) two-equation (k - ϵ) turbulence model for predicting the mixing time under these conditions; and (2) the extent to which the mixing time depends on the room airflow, rather than the source location within the room. The CFD simulations modeled the twelve mixing time experiments performed by Drescher et al. (1995) using a point pulse release in an isothermal, sealed room mechanically mixed with variable power blowers. Predictions of mixing time were found in good agreement with experimental measurements, over an order of magnitude variation in blower power. Additional CFD simulations were performed to investigate the relation between pollutant mixing time and source location. Seventeen source locations and five blower configurations were investigated. Results clearly show large dependence of the mixing time on the room airflow, with some dependence on source location. We further explore dependence of mixing time on the velocity and turbulence intensity at the source location. Implications for positioning air-toxic sensors in rooms are briefly discussed.

Keywords: mixing time, pollutant dispersion, CFD modeling, short-term exposure

1. Introduction

Indoor air quality investigations usually assume a uniform distribution of pollutants throughout each interior space. For experimental purposes, the assumption of instantaneous mixing justifies measuring concentrations at only one point in a room. In modeling studies, the well-mixed assumption simplifies the governing equations, producing systems of ordinary differential or even algebraic equations, rather than the partial differential equations that one must solve in order to account for real mixing.

However, the well-mixed assumption proves too simplistic for the initial period of the mixing of a pollutant in the room air, particularly for point sources and short-duration exposures. Furthermore, rooms may not become well-mixed over any length of time. For example, Lambert *et al.* (1993) showed that the levels of respirable suspended particles and nicotine were respectively 40% and 65% lower in no-smoking sections of restaurants than in the smoking sections. Thus the mixing problem has two aspects: (1) how to determine when the well-mixed approximation is inappropriate, and (2) how to model pollutant concentrations when the well-mixed approximation is inappropriate.

The concept of *mixing time* addresses the first question, of when one may safely apply the well-mixed assumption. For a point pulse release of pollutant in the room, under particular flow conditions, the mixing time defines the earliest point after which the room concentration is essentially uniform. Mixing time is intricately linked to whether one can simplify the estimation of exposure to a point pulse release of a pollutant. If the duration

of occupation in the room is many times longer than the mixing time, then a well-mixed approximation could be used for estimating the exposure and health effects for a point pulse release of the pollutant in the space. On the other hand, a duration comparable to, or shorter than, the mixing time suggests that a more detailed analysis is necessary to estimate exposure and health effects. Experimental work by Baughman *et al.* (1994) and Drescher *et al.* (1995) measured the mixing time for rooms under natural and forced convection, respectively.

Previous work on modeling imperfectly-mixed pollutants includes the introduction of a mixing factor, which represents the fraction of ventilation air that is completely mixed in the room (Ishizu, 1980). More recently, a multi-compartment model was applied, defining the space to be divided into several compartments, including a small virtual space around the source (Ozkaynak *et al.* 1982, Furtaw, 1996). This model gives each virtual zone a uniform concentration, but in principle it can be different from that in other zones in the room. Although this construction allows for initial concentration build-up near the source, comparisons with experiments show that concentrations near the source exceed the predictions of this modeling approach.

The current work focuses not on improving models of exposure under poorly mixed conditions, but on numerical investigation of the mixing time itself. Here we investigate whether it is possible to predict the mixing time numerically using the standard (k - ε) turbulence model, and the extent to which the mixing time depends on the source location. Specifically, we investigate: (1) the adequacy of the standard (k - ε) turbulence

model for predicting the mixing time of a point-source release; and (2) the extent to which the mixing time for a given room airflow is a characteristic of the airflow, rather than of the release location of the pollutant. Finally, we discuss implications of our findings for positioning sensors for acutely toxic pollutants in a room.

Much previous work applying CFD simulations to the contaminant dispersion in rooms was performed without corresponding experiments (Baker and Kelso, 1990). Yaghoubi *et al.* (1995) investigated mixing of pollutants using simulations with varied emissions from a pollutant source, cooling and heating locations, and incoming air temperatures. Roy *et al.* (1994) used a CFD code to predict contaminant dispersion in a kitchen-hood geometry.

Gadgil *et al.* (2000) provided a brief review of experimental and computational research investigations of pollutant dispersion in indoor spaces. Accurate CFD predictions of room airflow remains a demanding enterprise, requiring experience and care in defining the grid, treating boundary conditions, and selecting numerical properties of the model. Therefore, the present investigation includes comparisons to experiments that studied the mixing of a point pulse release of carbon monoxide (CO) in an isothermal, unventilated room with forced convection airflow. These comparisons validate the numerical treatment before extending the simulation results to the task of studying the relation between mixing time and source location. A part of this work was earlier reported by Lobscheid and Gadgil (2002).

2. Mixing time definition

Given a point pulse release of a pollutant in a room with no exhaust or fresh air supply, the pollutant will eventually be uniformly distributed throughout the room. If we denote the time elapsed after the point pulse release as t , then a characteristic mixing time, τ_{mix} , can be defined such that for t smaller than τ_{mix} , the pollutant concentration varies substantially throughout the room, and for t larger than τ_{mix} , the pollutant concentration is essentially uniform throughout the room. Imagine N monitoring points distributed in the room where pollutant concentration is being continuously monitored, each monitor recording a concentration $C_i(t)$. The mixing time is defined as the time at which the standard deviation of the $C_i(t)$ drops permanently below 10% of the arithmetic mean concentration $\bar{C}(t)$ of the pollutant at the monitoring points:

$$\text{For } t \geq \tau_{mix}, \quad \frac{1}{\bar{C}(t)} \sqrt{\frac{\sum_{i=1}^N (C_i(t) - \bar{C}(t))^2}{N}} \leq 0.10 \quad (1)$$

Of course, N must be sufficiently large, and the monitoring points sufficiently dispersed in the room, that additional monitoring points do not change the value obtained for the mixing time.

3. Experiment Description

Figure 1 presents isometric and plan views of the experimental room, which measured 3.53m x 3.74m x 2.36m high (31m³). Vertical edges of the room are denoted in the isometric and plan views for later discussion. Five identical, independently-controlled centrifugal fans were placed 3 cm above the ground. Each was fitted with a 60 cm long plastic exhaust pipe, positioned parallel to each other and to the floor. In each experiment, after the room airflow was established, 1.5 liter of pure CO was released into the unoccupied room over a period of 20 seconds through a perforated cylinder. The CO concentrations at nine fixed locations in the room were monitored, and the temperatures recorded at several other points. Each experiment was replicated once. An attempt was made to reach isothermal conditions in the room – such conditions were not attained exactly, and the experimenters applied a correction to remove the influence of natural convection from experimentally measured mixing time (both uncorrected and corrected values of mixing times are reported). The correction comprised subtracting the mixing time contributions of the residual natural convection assuming that the contributions from forced and natural convection added in the same manner as resistors in parallel (i.e., as reciprocal powers.) On analysis of corrected data, Drescher *et al.* (1995) determined that the mixing times could be well predicted by equation (2).

$$\tau_{mix} = c * \frac{M^{1/3} L^{2/3}}{P^{1/3}} \quad (2)$$

where c is the constant of proportionality, M (kg) denotes the mass of the air in the room, L (m) is a characteristic dimension of the room (in this case the height), and P (W) is the mechanical power deposited into room air. The term multiplying the constant c on the

right-hand side, is also known as power parameter p , and has units of time. The experimental data could be fitted with the equation:

$$\tau_{mix} = 0.29 p + 0.22 \quad (\text{experimental data}) \quad (3)$$

Detailed experimental descriptions can be found in Drescher (1994) and Drescher et al. (1995). It is important to note that the values of blower power and blower exhaust velocities spanned by the experiments were within ranges commonly encountered in the indoor environment.

4. CFD modeling

4.1 Grid and boundary conditions

Most of the room space was discretized with a coarse 10 cm X 10 cm X 10 cm mesh, except near the room boundaries and near the blower exhausts, where the grid was appropriately refined. A large inner block of cells enclosing the blowers was aligned with the exhaust pipes of the blowers, to avoid imposing the grid orientation on the exhaust jets. The blowers and attached pipes were simulated using block structures with 5 mm resolution at the ends of the blower pipes, where the highest velocities were expected. The walls of the room, as well as the outside surfaces of the blowers and pipes, were defined as impermeable non-slip boundaries. The blower inlets and exhausts were defined to have prescribed flows with fixed velocity profiles. The volume inside the blowers and exhaust pipes was excluded from the computational domain. The pollutant

concentration entering the blower inlet was imposed at the exhaust pipe outlet one time step later.

Good numerical predictions require a grid sufficiently refined that the CFD solution does not depend on the grid used. We recorded the steady-state velocities at a number of locations where the velocities were large or had large gradients (e.g., near the blower exhausts). The grids were successively refined until no significant changes in these velocities resulted. The final working grid was chosen to be the one from the penultimate of the successive refinement steps. This approach does carry a risk of missing important locations where further refinement would have made a measurable difference in the concentration field; hence the monitoring locations need to be carefully selected. Figure 2 presents a horizontal section, at 6 cm above the floor, of the final working grid of 130,942 nodes.

Predictions of transient pollutant dispersion must be independent of the time-step. We used a time step of 0.1 second for the simulation of pollutant dispersion in the “base-case” (all five blowers operating at an average exhaust air velocity of 1.86 m/s). Then we tested the predictions with those obtained using a 0.5 second and a 0.05 second time steps. The mixing time predicted with the small time step (0.05 s) was 198 seconds, and with the large time step (0.5 s) 196 seconds. These compared well with the predicted mixing time of 197 seconds of the simulation using 0.1 second time step. Therefore, this time-step was used for the other simulations.

4.2 Computational Procedure

The Navier-Stokes equations were solved with a commercial code based on a finite-volume fully-implicit method. We selected the standard (high Reynolds number) Reynolds Averaged Navier Stokes (RANS) two-equation (k - ε) model for turbulence. In an earlier separate (and unpublished) investigation, we determined that predictions using first-order upwind differencing gave unsatisfactory agreement with experimental observations; we found much improved agreement using the second-order MARS (Monotone Advection and Reconstruction Scheme) method which is superior in suppressing numerical diffusion. In the current investigation, only the MARS scheme was employed for both velocities and pollutant transport modeling. The Semi Implicit Method For Pressure Linked Equations (SIMPLE) algorithm was applied for the calculations of the steady-state velocity fields (Patankar 1980).

The chosen convergence criterion was that the sum of the residuals for all calculated dependent variables, at all the nodes, decreased below a value of 10^{-4} for the steady state calculations. Numbers of iterations to reach convergence for the steady state ranged from 1817 to 4855, requiring 10 to 35 hours processing time on a Sun Origin 2000 server with 2GB RAM and two processors. The transient calculations of pollutant dispersion (with the pre-calculated velocity field) required about half as much processing time.

Details of grid generation and testing, boundary conditions, time-step control, turbulence model parameters and computational procedure are described in Lobscheid (2001). For brevity, we skip writing out the steady-state incompressible Navier Stokes equations.

However, the standard k-e turbulence model equations with the model parameters employed in the simulations are shown below for completeness.

$$U_j \frac{\partial \varepsilon}{\partial x_j} = \frac{\partial}{\partial x_j} \left(\frac{\nu}{1.22} \frac{\partial \varepsilon}{\partial x_j} \right) + \frac{\varepsilon}{k} \left[1.44 \left(\frac{\partial U_i}{\partial x_j} + \frac{\partial U_j}{\partial x_i} \right) \frac{\partial U_i}{\partial x_j} \right] - 1.92 \frac{\varepsilon^2}{k} \quad (4)$$

$$\frac{\partial C}{\partial t} + U_j \frac{\partial C}{\partial x_j} = \frac{\partial}{\partial x_j} \left(D_{\text{molec}} + \frac{\nu_{\text{turb}}}{\sigma_m} \right) \frac{\partial C}{\partial x_j} \quad (5)$$

$$\nu = \nu_{\text{turb}} + \nu_{\text{molec}} \quad (6)$$

where

P is the pressure

U_i are the velocity components,

x_i are rectilinear orthogonal coordinates

k is the turbulent kinetic energy

ε is the dissipation rate of k

ν_{molec} is the molecular kinematic viscosity

ν_{turb} Nu-turb is the turbulent kinematic viscosity : $\nu_{\text{turb}} = 0.09k^2\varepsilon^{-1}$

The turbulent Schmidt number was assigned the value 0.9.

Additional computational details are as follows. The hydrodynamic diameters of the blower intake and exhaust were respectively 0.075 and 0.005 m; the source boundaries were 0.015m to the side, the turbulent intensity at the blower exhaust was specified to be

0.1, and the turbulent length at the blower exhaust was specified to be 0.1 times the diameter of the exhaust pipe.

5. Comparison of CFD results with experiments

In their experiments, Drescher *et al.* (1985) varied the mechanical power supplied by the blowers to the room air from 0.001 W to 0.985 W, and the experiments employed one or several blowers in different combinations operating at different power levels. In all configurations, the physical positions of the blowers remained fixed; only the power supplied to various blowers (in combination) was different. Temperatures at the walls and at different heights in the middle of the room were continuously monitored and found to differ from the average temperature by amounts ranging from 0.25 to 1.0 K with an average of 0.59 K. The influence of natural convection was neglected in the CFD simulations. Predictions are thus compared to the corrected mixing times measured and fitted by Drescher *et al.* (1995), equation (3) above.

Figure 3 shows the experimental data points and CFD predictions of mixing time as function of the power parameter p , spanning one order of magnitude. Compared to equation (3), the equation fitting the CFD predictions is:

$$\tau_{mix} = 0.23 p - 0.39 \quad (\text{CFD predictions}) \quad (7)$$

Figure 4 directly compares the pollutant mixing time predicted with CFD against those reported from experiments. The horizontal lines in the figure connect results of replicate experiments. On average, the two measurements made in each replicated experiment differed by 18%. The dashed line in Figure 4 indicates a perfect fit. Most of the points in Figure 4 lie below this line -- the CFD calculations underestimate mixing times by an average of 30%. This amount is large enough compared to the 18% average difference between replicate results to be significant, though it is small compared to the order-of-magnitude range spanned by the mixing times measured in the experiments (from 2.4 to 23 minutes). One possible reason for this general underprediction is that the flow fields in the room were not everywhere turbulent. Especially in cases where low blower power resulted in low air velocities (and long mixing time), parts of the room probably are laminar, for example in the middle of the room near the stagnation center of the bulk flow (see below). Therefore a low-Reynolds number k - ϵ model might be better at predicting the mixing times at the low end of the blower power range (i.e., at the high end of the mixing time range). As Heiselberg (1996) concluded, comparisons between measurements and CFD simulations at low air change rates will show large deviations if the numerical simulation does not take the low-Reynolds-number effects into consideration. The CFD work reported here did not explore predictions with a low-Reynolds-number model.

We investigated the influence on adding more pollutant monitoring locations on the calculation of mixing time. We examined simulations for 14 different blower configurations. The mixing time for these simulations spanned the full range explored

here (i.e., 100 to 1000 s). We calculated mixing time for each based on monitoring the pollutant concentrations at 9, 48, 100 and all (i.e., 130,942) locations. Results show about a 15% variability in the mixing times calculated with different number of monitoring locations, for any particular blower configuration. Note here that the 9 monitoring locations used by us were the same ones that Drescher *et al.* (1995) identified as sufficient. They based their analysis on previous mixing time measurements performed in the same room by Baughman *et al.* (1994) using 41 monitoring locations.

The CFD simulations permit a quantitative and detailed description of the airflow patterns in the room. One result of these airflow patterns, the mixing time, was measured experimentally by Drescher *et al.*, for one particular location of pollutant release. Since these airflow patterns will be relevant to understanding dispersion of pollutant released from other locations, it is instructive to briefly describe their major features, as understood with CFD.

The exhaust jets from the blower outlets run parallel to the floor, rapidly merging with one another, and entraining the room air as they move toward the east wall of the room. A part of this flow climbs the east wall, entraining more air as it slows down. This creates a large loop of air, in the vertical plane above the blowers, that is kept going by the main exhaust jets. This loop has an almost stagnant center about one meter above the blowers. Secondary recirculation loops are created as some of the air from the jets moves towards the south and north walls on reaching the east wall. A small stable loop is created in the lower SE corner that has relatively low air exchange with the main vertical

loop. Overall, the air velocities are high in the lower east edge of the room, and along the floor in the path of the jets. Velocities are much lower in the lower SW corner.

6. Impact of the pollutant source location on the mixing time

Additional simulations were performed to study the dependence of the mixing time on the location of the pollutant release. Five airflow configurations were chosen from the previous set of experiments to span the range of blower power (i.e., of average air velocity).

Seventeen pollutant source locations were investigated. The locations were selected considering two criteria:

- The locations should be possible points for a localized pollutant release (e.g., cigarettes, solvent chemical spills) in a room with no ventilation. This suggested investigating those locations where mail or boxes may be handled or opened (location height < 1.5m), and
- The set of locations should produce broad range of expected mixing-time values. Consequently, some sources would be located close to the blowers where the pollutant dispersion might be rapid (lower limit of mixing time range) and others in quiescent parts of the room (upper limit of mixing time range).

Figure 5 presents the 17 simulated pollutant source locations, the plan view of the computational grid, positions of the five blower exhausts, and the 48 monitoring points

in plan view. Twelve pollutant sources are located on the floor (four in the corners, four at the centers of the floor edges, and four in the central region of the floor, more than a meter from any wall). An additional five are located 0.75 meter high (in the core region of the room airflow, more than a meter from any wall), also shown in the plan view. Each source one liter in volume, roughly cubical, about 10 cm to the side (as allowed by the finite-volume grid). The sources on the floor have their lower surface resting on the floor.

We chose 48 evenly distributed locations within the room volume to record the evolution of local pollutant concentration during the CFD simulations of dispersion. Each location was centered in a 0.6 m^3 region in the room. These are also shown in Figure 5 in plan view. Ends of the blower exhaust pipes coincide with the bases of the arrows in Figure 5, with the direction of the arrow indicating the direction of the blower exhaust.

Figure 6 presents the predicted pollutant mixing time versus the average air speed in the room. Mixing times are plotted separately for sources in corners, floor edges, in the center region of the floor, and in the core of the room. On each graph, we also plot the mixing times predicted for the release location used in the Drescher et al (1995) experiments (hollow diamonds). These reference data, obtained by evaluating the concentration data at all 48 sensor locations, are provided for ease of comparison across graphs.

Figure 6 shows that the predicted mixing times for all source locations agree well with those calculated for a release from the reference location (points indicated with diamonds). Irrespective of release location, when the average air speeds in the room are high, the mixing times are short. Conversely, when the average room air speeds are low, the mixing times are long. The variability in the mixing time attributable to differences in the average room air speed is about a factor of 10. The scatter (or variability) arising from the source location is indicated by the vertical height of the band of points in the graphs. Across the whole range of air speeds, this variability remains about a factor of 2.

As may be expected, the mixing times are longer for pollutant sources located in the corners and at the edges of the room. The difference is especially prominent for low air speeds. For a given average room air speed, the mixing times for sources at corner or edge locations are longer than those for releases in the core by about a factor of 2.

At every air speed, a pollutant release in the SE corner of the room has the longest mixing time amongst all locations studied. This results from the air circulation loops described above. The closed loop in this corner causes the pollutant to circulate mostly locally, dispersing very slowly to other regions of the room. It is remarkable that this effect causes mixing times for releases in the SE corner to consistently exceed even those for release location with the lowest local air speeds (the SW corner).

7. Mixing time versus local air characteristics at source

The previous section shows that the average air speed dominates the mixing time calculation. For a given air speed, there is a smaller but still significant effect due to the source location. Comparing releases in the SE and SW corners, this effect may depend more on the overall circulation pattern than on the local air speed at the source. In general, once the pollutant reaches either the inlet region of the blowers, or gets entrained in the jets coming out of the blowers, rapid mixing thereafter is assured. (Determining the time for a significant fraction of the pollutant to reach the blowers zone is feasible with detailed knowledge of the three dimensional air flow patterns. However, this approach does not yield useful insights generalizable to practical situations for other room geometries and other air supply configurations.)

This section investigates the extent to which *local* flow characteristics at the source location can predict mixing time. Since pollutant dispersion away from the release point is driven by advection and turbulent diffusion, we consider both air velocity and turbulence. If advection and turbulent diffusion are locally strong, the pollutant will quickly disperse away from the source and perhaps enter the general circulation in the room. Figures 7 and 8 respectively show pollutant mixing time as a function of air speed and turbulence intensity at the source location.

Turbulence intensity at any point is defined by:

$$I = \frac{\sqrt{\frac{2}{3}k}}{U} \quad (8)$$

where I is the turbulent intensity (dimensionless), k is the local turbulent kinetic energy (m^2/s^2), and U is the local velocity magnitude (m/s).

Figure 7 shows that the pollutant mixing time is short if air velocity at the source is higher than about 0.15 m/s. This applies, for example, for source locations in the path of the exhaust jets from the blower. However, if the air velocity is lower than 0.15 m/s, mixing time values are scattered – the mixing times can be long or short depending on the local flow details. For example, the region upstream of the blower inlets has relatively low velocities, but the mixing time for releases from that region are short (owing to entrainment into the blower intake flow and subsequent high speed ejection from the exhaust). On the other hand, air speeds are relatively low in other corners and produce long mixing times.

We can only speculate on the extent to which this value of about 0.15 m/s will change for rooms of other sizes and with other air supply configurations. Air speeds of this magnitude are commonly found in rooms, for example in thermal plumes and in entrained jets from supply vents. Larger rooms of roughly equal heights do not exhibit proportionally larger indoor air speeds. This suggests that the value of 0.15 m/s might not change substantially for various sizes of ordinary rooms.

Figure 8 plots mixing time against turbulence intensity at the source. The points are widely scattered, and it is difficult to see general trends in the figure. Taken together, Figures 7 and 8 suggest that locally high air speed is a better predictor of short mixing

time than locally high value of turbulent kinetic energy. In other words, advection, rather than turbulent diffusion, is the locally dominant mechanism in situations with short mixing time. This makes sense given that real rooms (such as the one modeled in this paper), unlike stirred tank chemical reactors, have low turbulent intensities, and therefore low turbulent diffusivities. We discuss in the next section implications of this for positioning indoor sensors for detecting toxic airborne threats.

8. Discussion and Conclusion

In this study, we predicted mixing time for a point pulse release of a pollutant for a mechanically mixed isothermal room, using the standard (k - ε) turbulence model, implemented with the MARS solution algorithm, and carefully implemented grid and boundary conditions. The predictions were found to be within 30% of experimental measurements for a range of conditions that span one order of magnitude in mixing time.

We explored the mixing times for 17 different release locations and five settings of blower power, spanning a realistic range of mechanical power supplied to room air in real buildings. Pollutant mixing time was found to depend primarily on the mean airflow in the room, and secondarily on the pollutant source location. For a given airflow in the room, mixing times for sources located near the walls (in the corners and at the edges of the room) are about twice as high as for those located in the core region. Predictions of mixing time can be made based on the local air velocity at the source location only for

high air velocity (greater than about 0.15 m/s). Turbulence intensity at the source location is poorly correlated to the pollutant mixing time.

In this study, we simulated many sensors positioned in the room, and based on the concentrations at the simulated sensor-locations, investigated whether, and how, source location might influence pollutant mixing time in a room. One might pose the inverse question. What do these findings about source locations and mixing times suggest about positioning an air-toxics sensor in a room. The desirable attribute of a sensor-location is that an airborne pollutant released in a room should reach that location quickly. Sensors should not be placed at locations where sources have long mixing times (e.g., corners or edges of a room). This is because long mixing times suggest that either the air there is stagnant, or it flows within a local recirculating loop --- characteristics that will cause delayed sensing of a pollutant by sensors placed at these positions. Conversely, the locations from which a source disperses quickly into the room (e.g., behind a table fan) would also be desirable locations for sensors for quick detection. This argument of course needs to be modified for real rooms, which typically have registers for air supply and return (i.e., exhaust). At one extreme, pollutant released near the room air return register may not mix in the room at all, and a sensor located at the fresh air inlet may never detect a toxic substance released in the room. Exchange of air from the room to the outside breaks the symmetry between source and sensor locations. However, supply and exhaust registers are not the only cause of room air mixing. Mixing from natural convection (Baughman et al. 1994), mechanical devices such as table fans (Drescher et al. 1995), and occupant movement (Mora and Gadgil 2002) can produce good mixing and

short mixing times. Thus we suspect that the broad conclusions suggested in this paragraph will retain some validity even in the presence of ventilation supply and exhaust. Nevertheless, further investigation is needed to elucidate this matter and develop general principles.

Acknowledgements

The authors are grateful to Anushka Drescher for generously sharing detailed experimental data from the CO mixing experiments, and David Lorenzetti for his helpful editorial comments. This work was supported by the Office of Nonproliferation Research and Engineering, Chemical and Biological National Security Program, of the National Nuclear Security Administration under U.S. Department of Energy Contract No. DE-AC03-76SF00098.

References

- BAKER, A.J., and KELSO, M. (1990) "On validation of computational fluid dynamics procedures for room air motion prediction", *ASHRAE Transactions*, **96**(1), 760-774.
- BAUGHMAN, A.V., GADGIL, A.J., and NAZAROFF, W.W. (1994) "Mixing of a point source pollutant by natural convection flow within a room", *Indoor Air*, **4**, 114-122.
- DRESCHER, A.C. (1994) *Computed Tomography and Optical Remote Sensing: Development for the Study of Indoor Air Pollutant Transport and Dispersion*, Ph.D. Thesis, Dept. of Civil and Environmental Engineering, University of California, Berkeley.

DRESCHER, A.C., LOBASCIO, C., GADGIL, A.J., *et al.* (1995) “Mixing of a point source indoor pollutant by forced convection”, *Indoor Air*, **5**, 204-214.

FURTAW, J., PANDIAN, M.D., NELSON, D.R., *et al.* (1996) “Modeling indoor air concentrations near emission sources in imperfectly mixed rooms”, *Journal of Air and Waste Management Association*, **46**, 861-868.

GADGIL, A.J., FINLAYSON, E.U., FISCHER, M.L., *et al.* (2000) “Pollutant transport and dispersion in large indoor spaces: a status report for the large space effort of the interiors project”, *Lawrence Berkeley National Laboratory Report*, **LBNL-44791**, Berkeley, USA.

HEISELBERG, P. (1996) “Room air and contaminant distribution in mixing ventilation”, *ASHRAE Transactions: Symposia*, 332-339.

ISHIZU, Y. (1980) “A general equation for the estimation of indoor pollution”, *Environmental Science & Technology*, **14**, 1254-1257.

LAMBERT, W.E., SAMET, J.M. and SPENGLER, J.D. (1993) “Environmental tobacco smoke concentrations in no-smoking sections of restaurants”, *American Journal of Public Health*, **83**, 1339-1341.

LOBSCHIED, C. (2001) *Isothermal mixing of a point source indoor pollutant: numerical predictions and comparison with experiments*, Diploma Thesis, Faculty of Process Engineering, Hermann-Rietschel Institute, Technical University of Berlin, Germany.

LOBSCHIED, C., and GADGIL, A. J. (2002), “Mixing of a point-source indoor pollutant: numerical predictions and comparison with experiments,” Proceedings, Indoor Air 2002, **IV**, pp. 223-228. Also Lawrence Berkeley National Laboratory Report **LBNL-49457**.

Mora L., and Gadgil, A. J., (2002), “Theoretical study of pollutant mixing in rooms induced by occupancy,” Proceedings, RoomVent 2002, Copenhagen, Denmark. Also, Lawrence Berkeley National Laboratory report **LBNL-49730**.

OZKAYNAK, H., RYAN, P. B., ALLEN, G. A., AND TURNER, W. A., (1982), “Indoor Air Quality Modeling: Compartment Approach with Reactive Chemistry”, *Environment International*, **8**, 461-471.

PATANKAR, S. V. (1980) *Numerical Heat Transfer and Fluid Flow*. Hemisphere Publishing, McGraw-Hill, New York.

ROY, S., KELSO, R.M., and BAKER, A.J. (1994) “An efficient CFD algorithm for the prediction of contaminant dispersion in room air motion”, *ASHRAE Transactions*, **100**(2), 980-987.

YAGHOUBI, M.A., KNAPPMILLER, K.D., and KIRKPATRICK, A.T. (1995) “Three-dimensional numerical simulation of air contamination dispersal in a room”, *ASHRAE Transactions*, **101**(2), 1031-1040.

Figure Captions

Figure 1. Schematic of the experimental room (isometric and plan views). Stars represent CO sensors.

Figure 2. Plan view of the final computational grid, shown at a height of 6 cm above the floor of the room.

Figure 3. Mixing times as a function of the power parameter, p , for experiments and simulations. Experimental values shown are after correction by the experimenters for the small effect of natural convection.

Figure 4. Comparison between experimental measurements and numerically predicted mixing times. Each experiment was replicated once, and both the experimental measurements are shown.

Figure 5. Seventeen simulated pollutant source locations, 16 of the 48 monitoring locations, and exhaust jet locations from the blowers, shown in plan view. Each pollutant source location on the floor is shown as a solid rectangle. On the floor, four sources are seen at the centers of the edges, denoted by Edge_01 to Edge_04, four in corners, denoted by Corner_01 to Corner_4, and four in the mid-area, denoted by Floor_01 to Floor_04. Five source locations at a height of 0.75m are indicated in the plan view by vertical hatched rectangles, and identified as Core_01 to Core_05. The monitoring locations, marked with "S", are arranged in sixteen stacks of three locations each, one in each of three horizontal planes at heights 0.4m, 1.2m and 2.0m above the floor. The plan view shows the monitoring locations in one horizontal plane. The monitoring locations are connected with a 4X4 grid for ease of identification. Bases of arrows coincide with the

ends of the five blower exhaust pipes. The grid for the computational domain at mid-height in the room is also shown in plan view.

Figure 6. Mixing time for sources in the corners, floor edges, floor center region, and room core, as a function of average room air speed. Note the vertical axis is logarithmic. On the log axis, the vertical scatter of the points is roughly the same at each value of average room air speed; showing that the ratio of the highest to the lowest mixing time is roughly the same.

Figure 7. Mixing time versus local air speed at the source location. The plot symbols show different average room air speeds, as determined by the different blower powers. Whenever the local air velocity exceeds about 0.15 m/sec, the mixing time is invariably short. See text.

Figure 8. Mixing time versus air turbulent intensity at the pollutant source location. The five different symbols represent five different blower power configurations. These are keyed in the figure caption box by the average room air velocity, which spans an order of magnitude.

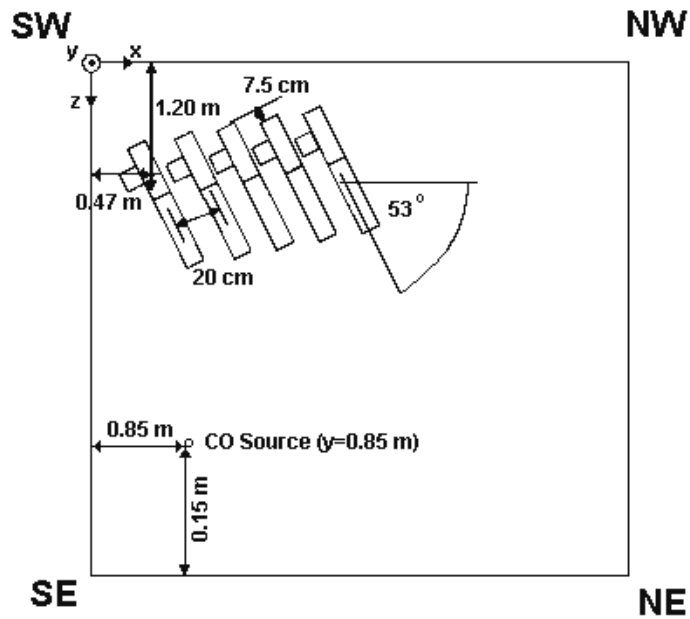
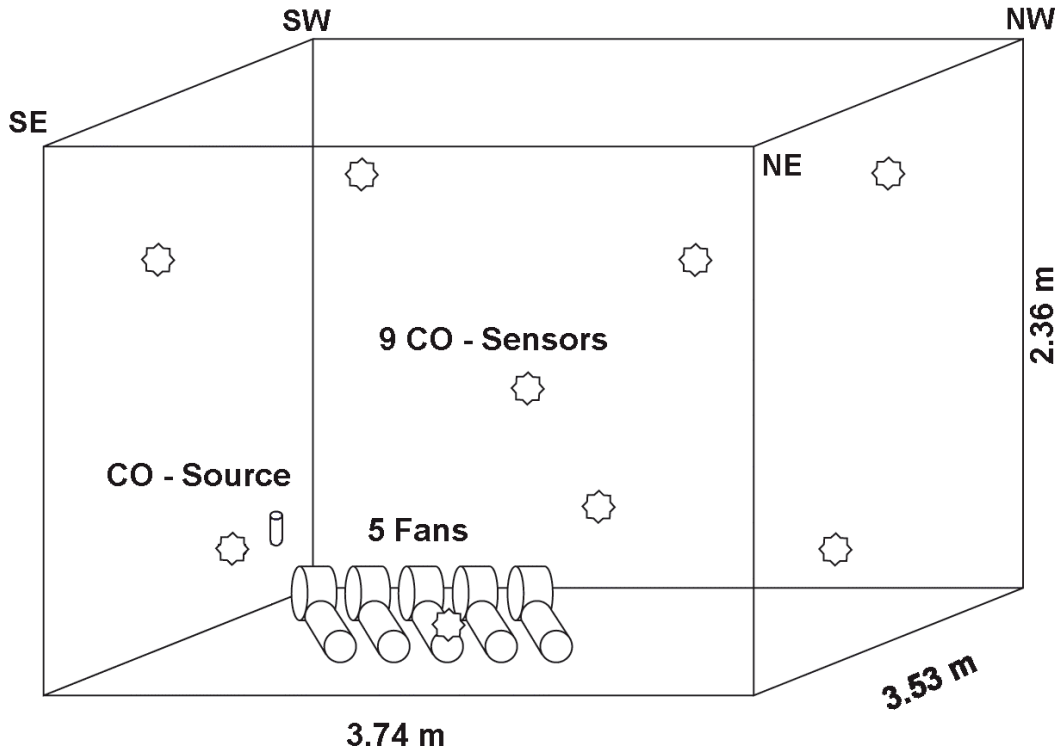


Figure 1

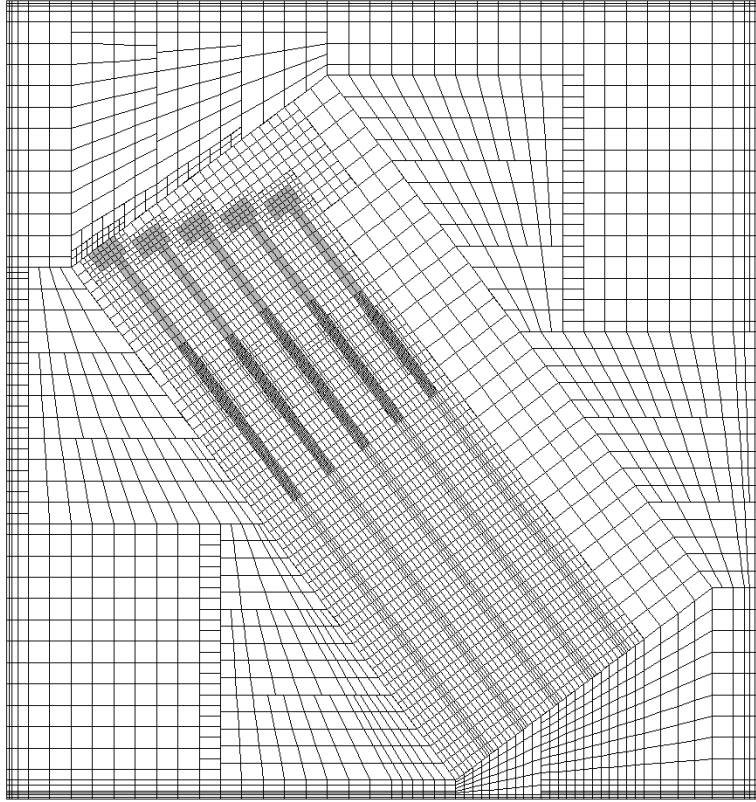


Figure 2

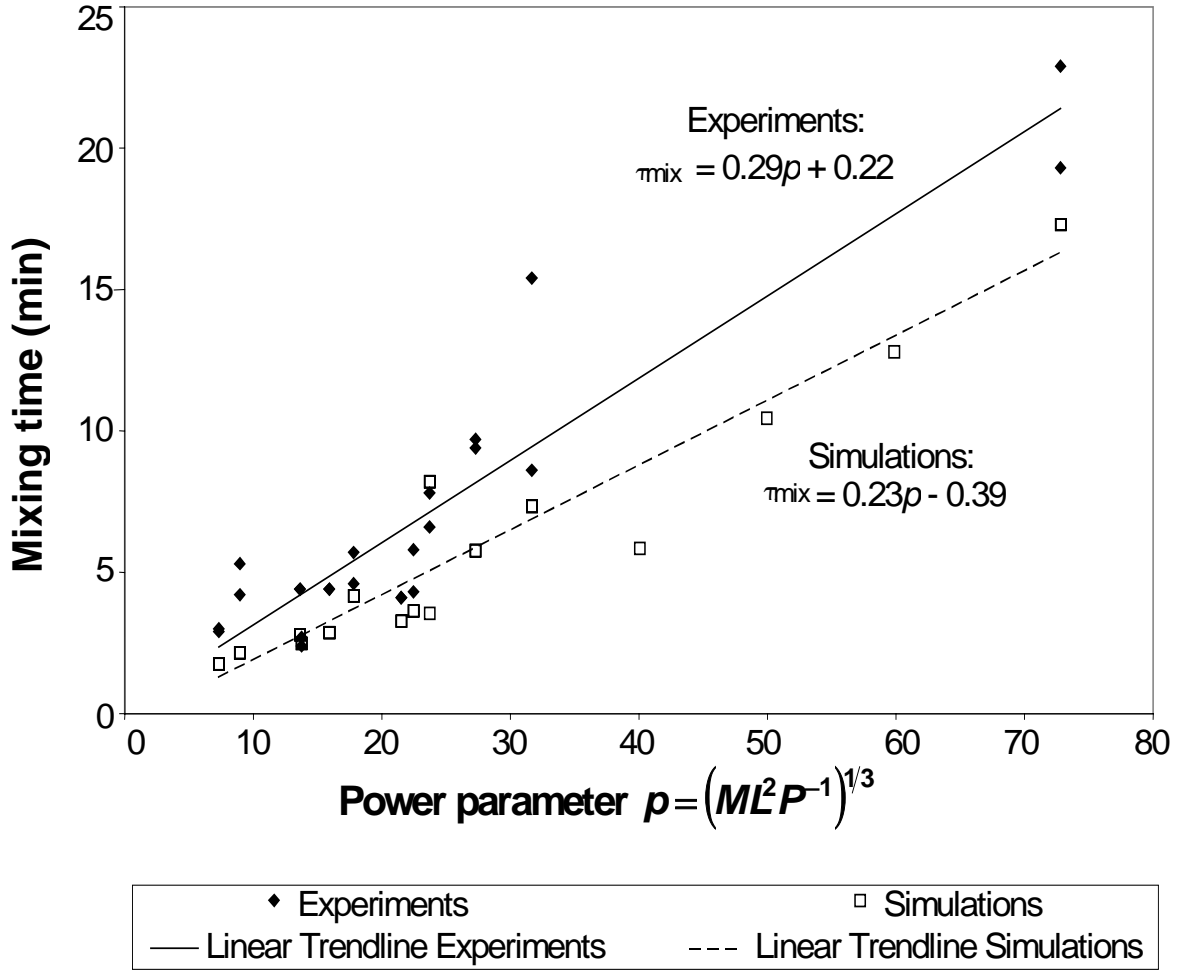


Figure 3

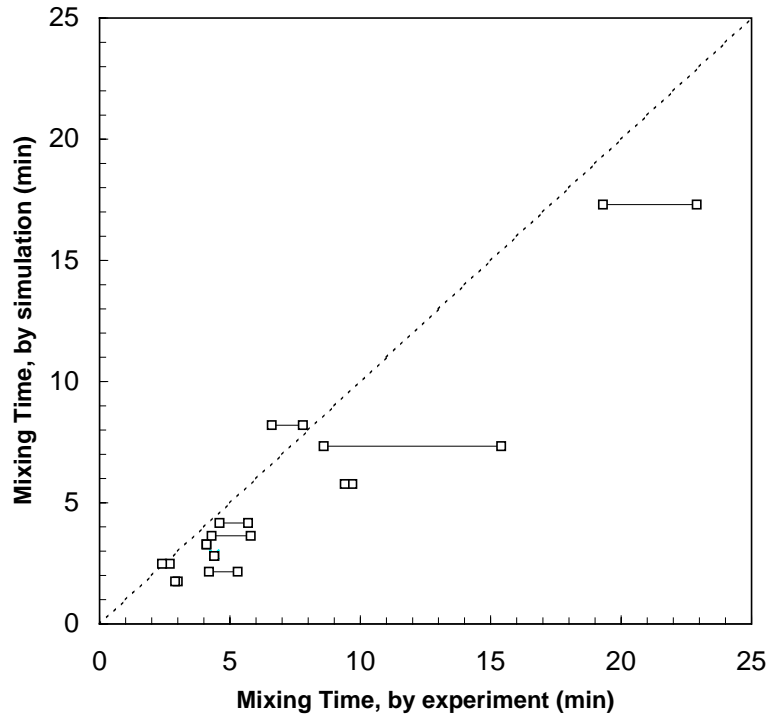


Figure 4

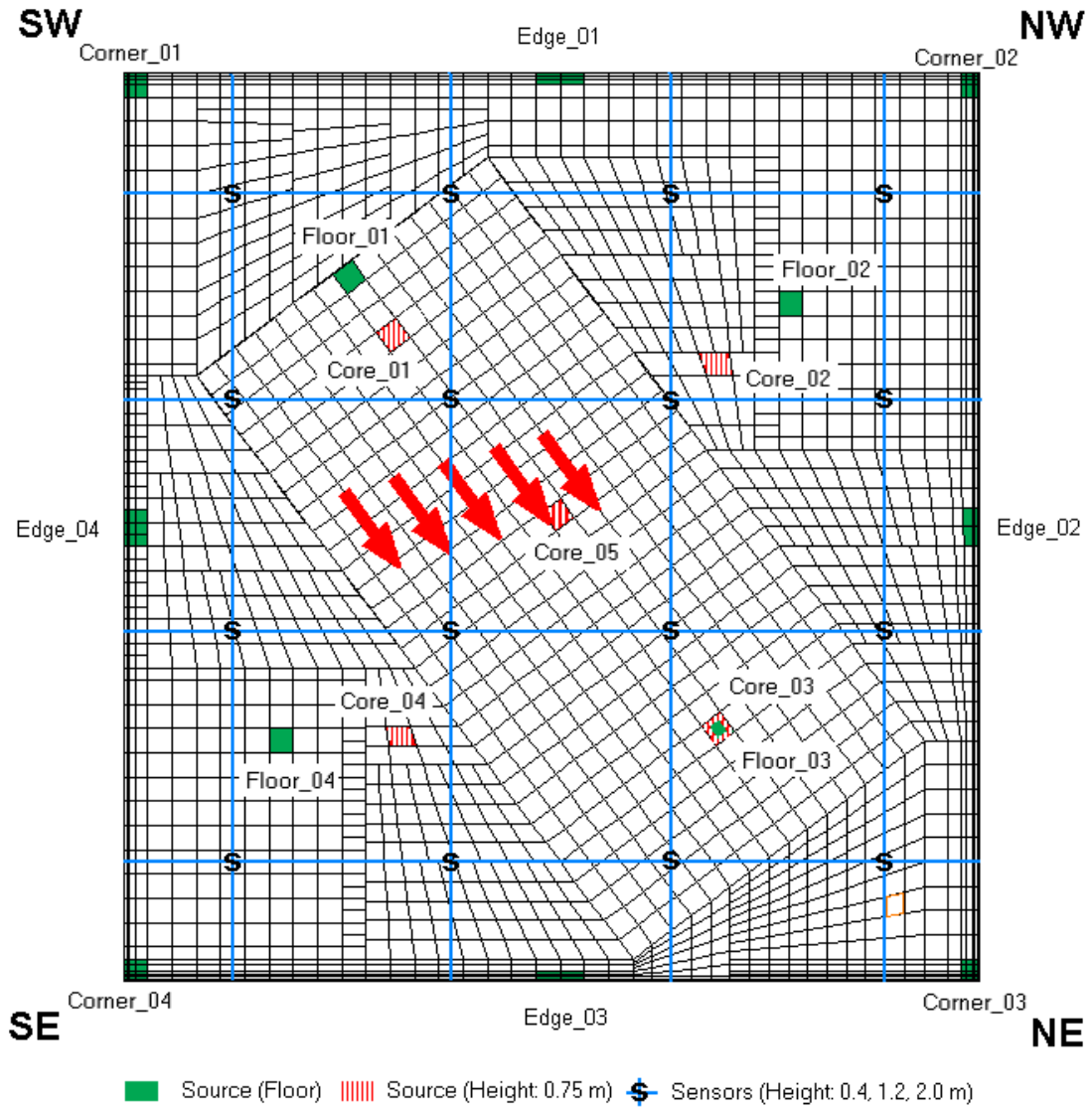


Figure 5

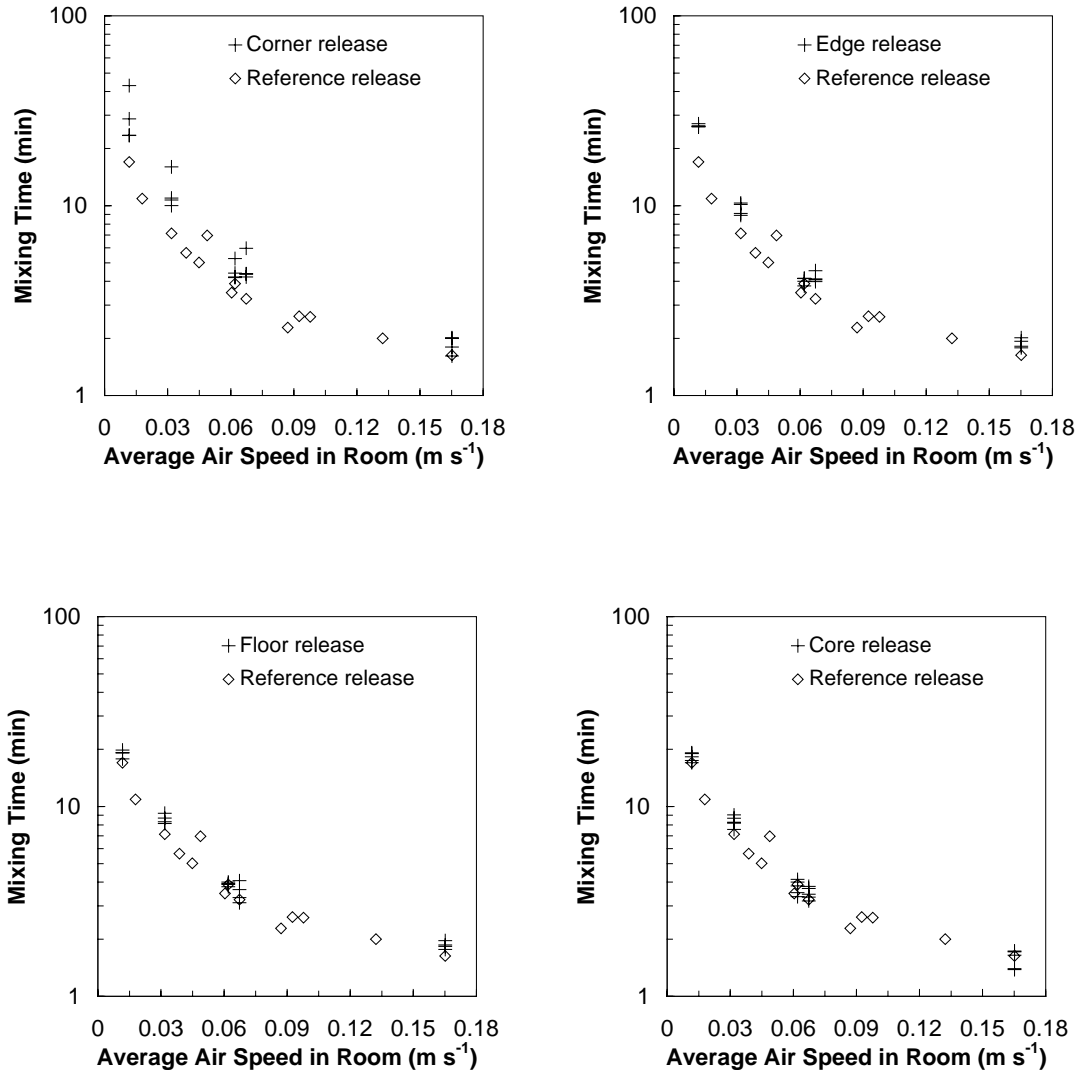


Figure 6

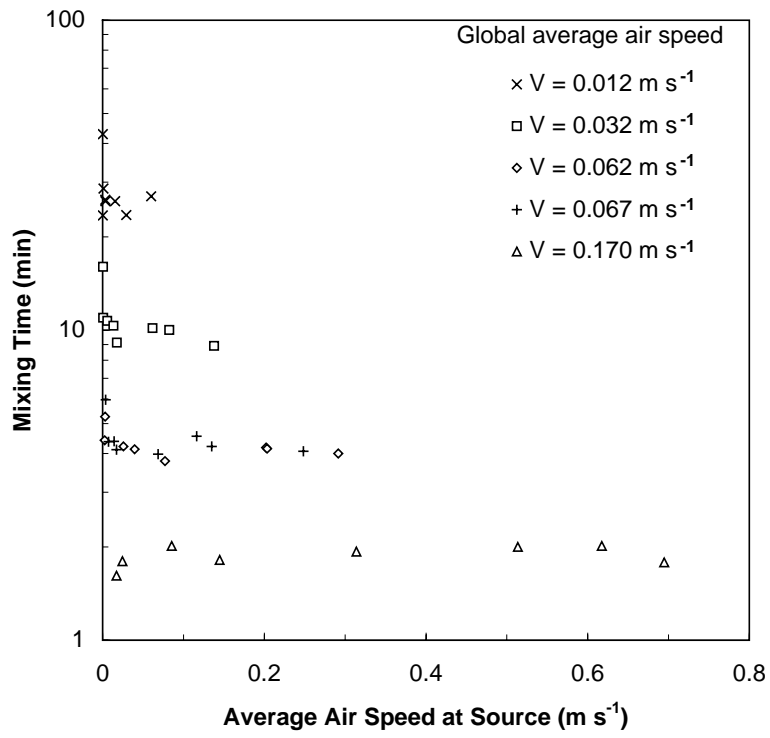


Figure 7

